

Impact of Urbanization on Land Surface Temperature Using Deep Learning Approach

Manikandan Sathianarayanan (1), Dr, Pai-Hui Hsu (2)

^{1,2}Dept. of Civil Engineering, National Taiwan University, Taiwan

Email: d06521026@ntu.edu.tw ; hsuph@ntu.edu.tw

Abstract: Land use change and urbanization are the two astonishing factors can introduce ambiguity to the estimation of global temperature trends related to climate change. In this work, we investigate the characteristics of urban expansion and its impact on land surface temperature using a time series of Landsat images. Accurate land cover information required in order to relate land surface temperature with land cover features. Even with increased number of satellite systems and sensors acquiring data with improved spectral, spatial, radiometric and temporal characteristics of remotely sensed image with an ambiguous accuracy. One major approach for improving accuracy is to develop an accurate and effective image classification algorithm. This work incorporates a long short-term memory (LSTM) recurrent neural network (RNN) model to take advantage for time series images to improve accuracy and reduce complexity. Network trained thoroughly using state of the art techniques of deep learning and finally, we tested our model on multiple Landsat images to derive urban land cover changes (ULCC). Then, Land surface temperature has been calculated from thermal data of Landsat TM/TIRS using emissivity derived from NDVI images. Urban density as a measure of urbanization has been derived from gravity model. Later, land surface temperature data associated with land use and land cover information for further investigation of the relationship between land surface temperature behavior with land cover features. The results provide a scientific reference for policy makers and urban planners can work towards a sustainable and healthy environment.

Keywords: LSTM, RNN, LST, NDVI, ULCC

Introduction:

Land cover refers to the pattern of ecological resources and human activities dominating different areas of the Earth's surface. It is a critical type of information supporting various environmental science and land management applications at global, regional, and local scales (Foley et al., 2005; Meyer & Turner, 1994). Given the importance of land cover information to global change and environmental sustainability research, there have been numerous efforts aiming to derive accurate land cover datasets at various scales mostly by using various remote sensing technology. However, even with the increased number of satellite systems and sensors acquiring data with improved spectral, spatial, radiometric and temporal characteristics and the new data distribution policy, most existing land cover datasets were derived from a pixel-based single-date multi-spectral remotely sensed imagery using conventional or advanced pattern recognition techniques such as random forests (RFs) (Shi & Yang, 2016), neural networks (NNs) (Kavzoglu & Mather, 2003; Mas & Flores, 2008) and support vector machines (SVMs). A major bottleneck is an accurate and effective image classification technique which can incorporate and utilize multi-spectral, multi-temporal and spatial information available to derive land cover datasets from remote sensing images.

Urban land cover changes (ULCC) due to urbanization are mainly caused by removal of vegetation cover, which affects the surface climate. When the surfaces of different materials receive the same amount of solar radiation, the resulting temperature differs due to differences in their heat capacity. Land surface temperature (LST) is an important indicator of urban climate. Due to urban areas' surface cover, surface temperature is higher than in vegetated and water-covered areas. Accordingly, the increasing number of built-up areas results in increased temperature values. It is important to study the impact of urbanization on LST, since it can disrupt a wide range of natural processes. Using remote sensing for studying climate variables has become popular, especially with the introduction of thermal remote sensing. However, a historical construction of the relationship is needed in order to reach reliable conclusions. To address this, one study used 507 Landsat Thematic Mapper (TM)/Enhanced Thematic Mapper Plus (ETM+) images from 1990 to 2018. This attempt found it challenging to automatically characterize ULCC consistently at an acceptable accuracy. In this paper we assess the use of deep neural networks to consider the temporal correlation of the data. In fact, through recent advances in machine learning, there has been an increased interest in time series classification using deep convolutional neural networks (CNNs) and recurrent neuron networks (RNNs) that can take advantage of neural networks for end-to-end classification of a time series. Moreover, RNN approaches can be used to work on pixel-based time series. Accordingly, we focus our attention on RNN approaches for the classification.

Thanks to their property, RNNs offer models to explicitly manage temporal dependencies among data (e.g., long short term memory (LSTM) and Gated Recurrent Unit (GRU)), which makes them suitable for the mining of multitemporal SAR Sentinel-1 data or Landsat series of images.

The objective of this work is to evaluate the potential of high spatial and temporal resolution of Landsat remote sensing data to: (i) Map different agricultural land covers; and (ii) assess the new deep learning technique by comparing it with the standard machine learning approaches, (iii) make relationship between land surface temperature and land cover features.

Datasets

In this study, the main data sets were time series of Landsat images taken by the Landsat TM, Landsat ETM+, and Landsat Operational Land Imager (OLI)/Thermal Infrared Sensor (TIRS) sensors, and obtained from the USGS website (<https://earthexplorer.usgs.gov>). Satellite images were obtained with 3–4-year intervals, and within the same season (the dry season) to avoid phenological variations. The software used to conduct image processing included Environment for Visualizing Images (ENVI), ArcGIS 10.5. Pre-processing was done for the Landsat images as it can have a great impact on the results of the analysis. Usually, it is not necessary to conduct a geometric correction for Landsat level 1 products, as they are registered and ortho-rectified through a systematic process.

Table 1. Information about Landsat image used in this study.

ID	Sensor Type	Acquisition data	Path/Row	Spatial resolution
LT05_L1TP_117043_19951125_20170106_01_T1	TM	11/25/1995	117/43	30 m
LE07_L1TP_117043_20000927_20180429_01_T1	ETM	9/27/2000	117/43	30 m
LE07_L1TP_117043_20050909_20170113_01_T1	ETM	9/9/2005	117/43	30 m
LE07_L1TP_117043_20101228_20161211_01_T1	ETM	12/28/2010	117/43	30 m
LC08_L1TP_117043_20180313_20180320_01_T1	OLI_TIRS	3/13/2018	117/43	30 m

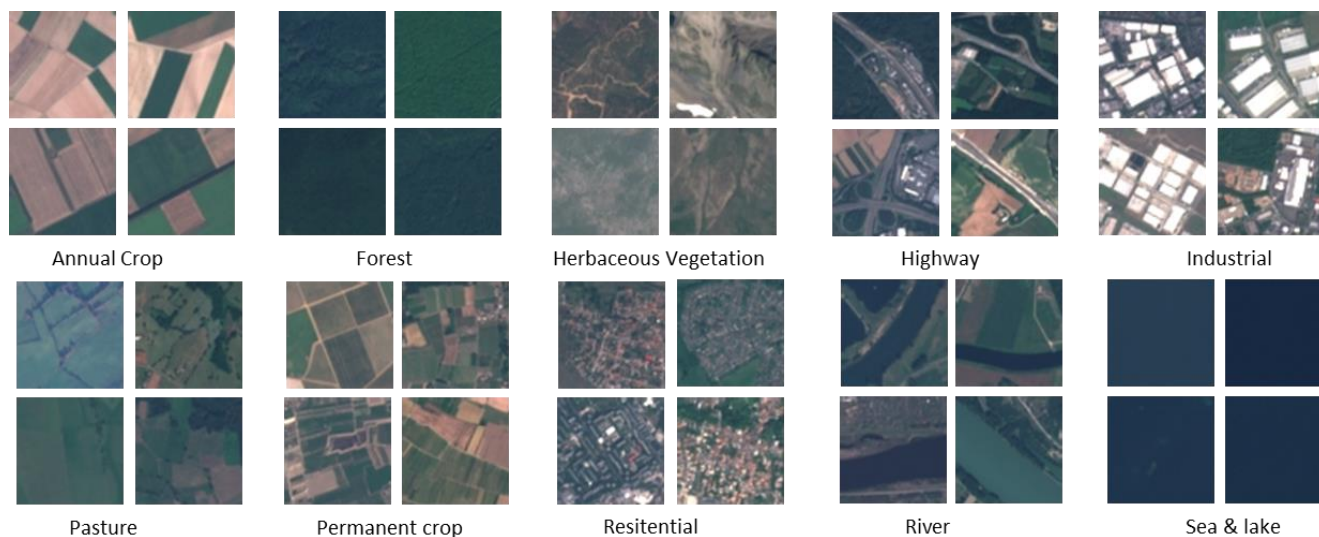


Fig 1. Sample images from EuroSAT dataset

The Sentinel-2 satellite constellation provides about 1.6 TB of compressed images per day. Unfortunately, supervised machine learning is restricted even with this amount of data by the lack of labeled ground truth data. The generation of the benchmarking EuroSAT dataset was motivated by the objective of making this open and free satellite data accessible to various Earth observation applications and the observation that existing benchmark datasets are not suitable for the intended applications with Sentinel-2 satellite images. The dataset consists of 10 different classes with 2,000 to 3,000 images per class. In total, the dataset has 27,000 images. The patches measure 64x64 pixels. We have chosen 10 different land use and land cover classes based on the principle that they showed to be visible at the

resolution of 10 meters per pixel and are frequently enough covered by the European Urban Atlas to generate thousands of image patches. EuroSAT dataset was very useful for land use land cover classification using LSTM RNN networks through transfer learning of VGG-16 model.

Long-Short Term Memory (LSTM):

The existing RNN models fail to learn long-term dependencies because of the problem of vanishing and exploding gradients. To overcome this challenge, the LSTM model is used by Hochreiter, S.; Schmidhuber, J 1996.. The Equations (1)–(6) formally describes the LSTM neuron. The LSTM set consists of two cell states: The C_t memory and the h_t hidden state. Three different gates intervene in the control of the flow of information: The input (i_t), the forget (f_t) and the output (o_t). All three gates mix the current entry, x_t , with the hidden state, h_{t-1} , from the previous timestamp. Also, the gates have two major functions: (i) They regulate the quantity of information to forget/remember during the process; (ii) they deal with the problem of gradient disappearance/bursting. We can see that the gates are implemented by a sigmoid. This function gives values between 0 and 1. The LSTM unit also uses a temporary cell state, y_t , that resizes the current input. This current cell is applied by a hyperbolic tangent function that gives values between -1 and 1. The sigmoid and the hyperbolic tangent work per element. it sets the amount of information to keep ($i_t \odot y_t$), while f_t indicates how much memory should be kept in the current step ($f_t \odot c_{t-1}$). The input of an RNN is a sequence of variables (x_1, \dots, x_n), where x_t is a generic element that represents a feature vector and t refers to the corresponding timestamp.

Finally, o_t has an impact on the new hidden state, h_t , which determines how much information from the current memory will be on the output step. The different matrices, W_{**} , and bias coefficients, b_{**} , are the parameters used during model formation. The memory, C_t , and the hidden state, h_t , are both transmitted at the next step.

$$i_t = \sigma(W_{ix}x_t + W_{ih}h_{t-1} + b_i)$$

$$f_t = \sigma(W_{fx}x_t + W_{fh}h_{t-1} + b_f)$$

$$y_t = \tanh(W_{yx}x_t + W_{yh}h_{t-1} + b_y)$$

$$c_t = i_t \odot y_t + f_t \odot c_{t-1}$$

$$o_t = \sigma(W_{ox}x_t + W_{oh}h_{t-1} + b_o)$$

$$h_t = o_t \odot \tanh(c_t)$$

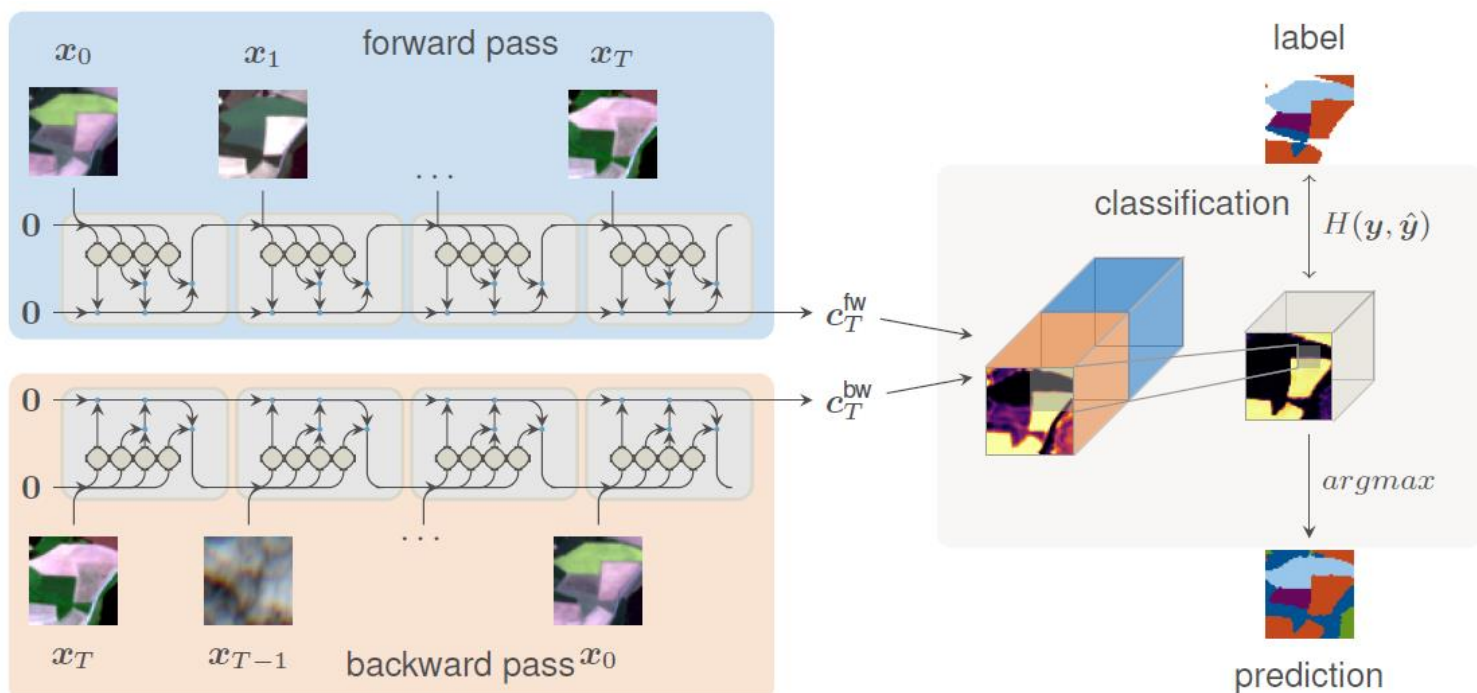


Fig 2. Schematic illustration of our proposed bidirectional sequential encoder network. The input sequence $x \in \{x_0, \dots, x_T\}$ of observations $x_t \in R^{h \times w \times d}$ is encoded to a representation $c_T = [C_T^{seq} || C_0^{inv}]$. The observations are passed in sequence (seq) and reversed (rev) order to the encoder to eliminate bias towards recent observations. The concatenated representation of both passes c_T is then projected to softmax-normalized feature maps for each class using a convolutional layer. (Rußwurm M., Körner M. (2018).

Land Surface Temperature Estimation

In the literature, numerous studies can be found on methods for calculating LST using Landsat images. The Mono–Window algorithm(Qin et al., 2001) ,the radiative transfer equation(Sobrino, et al.,2004), and the Single–Channel algorithm (Jimenez-Munoz et al., 2003) are some of the commonly known methods. However, these methods require additional input parameters (such as atmospheric water vapor content and near-surface air temperature) from ground-based observations, captured simultaneously with the satellite passes, and these are usually unavailable. For this reason, the method developed by number of researcher which necessitates no additional input parameters, was chosen for this research. All the digital numbers (DN values) of thermal bands corresponding to the classification year were converted into spectral radiance. Then the effective at-sensor brightness temperature is also calculated.

Effective at-Sensor Brightness Temperature

The equation for calculating the brightness temperature equation below is the same for Landsat TM, ETM+, and OLI/TIRS;

$$T = K2 / \ln\left(\frac{K1}{L\lambda} + 1\right)$$

where T is the effective at-satellite temperature (Kelvin), K1 is a calibration constant in W/(m2.sr. μ m), and K2 is another calibration constant in Kelvin.

Land Surface Emissivity Calculation

Knowledge of surface emissivity is important for land surface temperature calculations by remote sensing. In optical thermal remote sensing, there have been several studies on emissivity. Among these, we adopted the frequently used method with the calculation of emissivity using simplified normalized difference vegetation index (NDVI) thresholds, derived from the spectral reflectance in the red and near infrared bands. In this method, it assumed that the surface is flat and homogenous. The conditional below Equation for emissivity calculation is as follows:

$$emissivity = \varepsilon_{v\lambda} PV + \varepsilon_{s\lambda}(1 - Pv) + C_\lambda$$

where ε_v and ε_s are the vegetation and soil emissivity, which in this study are 0.98 and 0.92, respectively; and C represents the surface roughness (C = 0 for homogenous and flat surfaces), taken as a constant value of 0.005

Land Surface Temperature Estimation

Using the above calculated emissivity and effective at-sensor brightness temperature, images were further used to derive LST using Equation developed by

$$LST = \frac{BT}{\left\{1 + W * \left(\frac{BT}{\rho}\right) * \ln(e)\right\}}$$

where LST is in Kelvin (K), BT is the at-sensor brightness temperature (Kelvin), $\rho = hc/\sigma$, σ = Boltzmann constant (1.38×10^{-23} J/K), h is Planck's constant (6.626×10^{-34} J/s), c is the velocity of light (2.998×10^8 m/s), and e is the emissivity.

Land surface Temperature calculation:

The LSTs calculated from the Landsat images as discussed in the methodology are presented in Figure below. It shows a clear gradient between the urban areas and rural areas from 1990 to 2018, and also illustrates the increase in temperature. This is mainly due to the fact that urban surface materials will have higher radiant temperatures. The land cover pattern also shows a similar gradient to the temperature values.

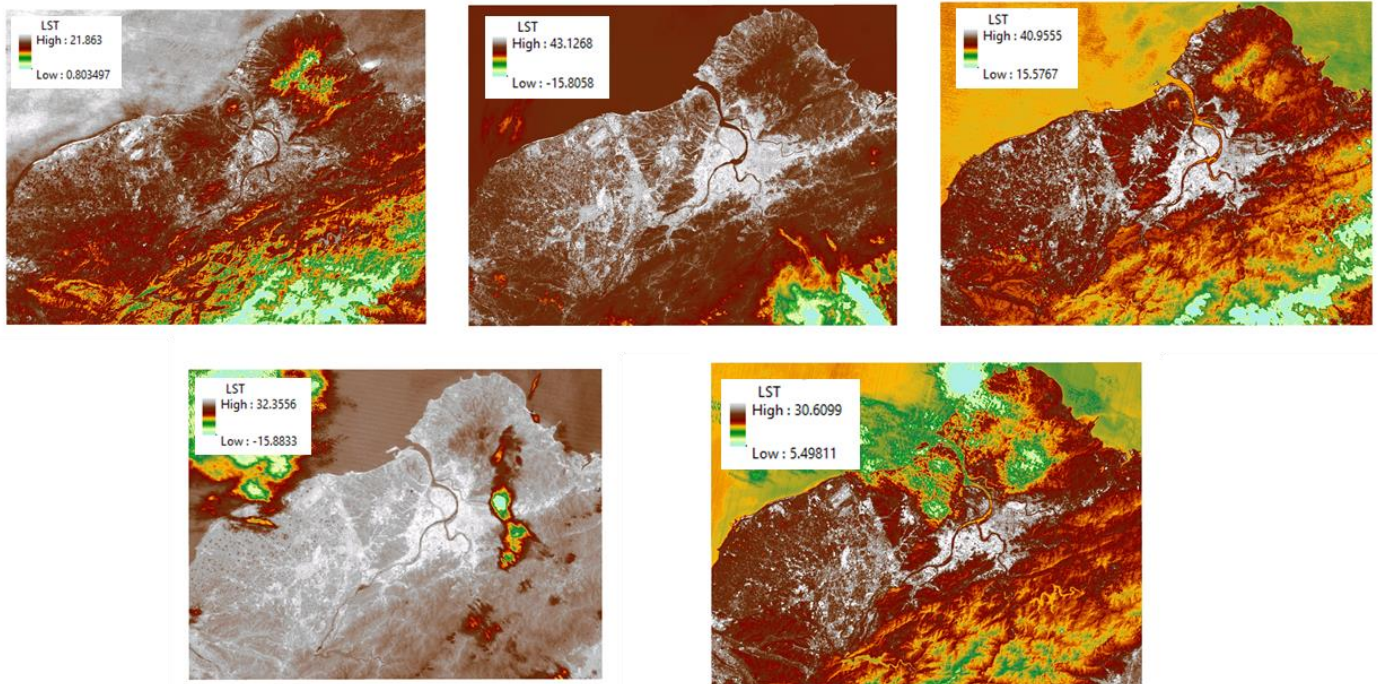


Fig 3. LST calculated images from 1995-2018

Conclusion and future work

In this paper, we studied potential of high spatial and temporal resolution of sentinel -1 remote sensing data for different agriculture land cover mapping applications and assessed through transfer learning and Long-short term memory recurrent neural networks. From a socio-economic perspective, cities are considered as magnets that attract people for various social and economic opportunities. Cities may attract or repel residents, money and business investment. To investigate the long-term changes of ULCC, and its impacts on thermal characteristics different methods should be employed such as gravity model or multiple buffer ring method. Since main consideration of this research is to identify the relationship between land cover features and LST values and LST values in the different land cover features should be extracted.

References

- Rußwurm, M.; Körner, M. Multi-Temporal Land Cover Classification with Sequential Recurrent Encoders. *ISPRS Int. J. Geo-Inf.* 2018, 7, 129.
- Ndikumana, E.; Ho Tong Minh, D.; Baghdadi, N.; Courault, D.; Hossard, L. Deep Recurrent Neural Network for Agricultural Classification using multitemporal SAR Sentinel-1 for Camargue, France. *Remote Sens.* 2018, 10, 1217.
- Fonseka, H.; Zhang, H.; Sun, Y.; Su, H.; Lin, H.; Lin, Y. Urbanization and Its Impacts on Land Surface Temperature in Colombo Metropolitan Area, Sri Lanka, from 1988 to 2016. *Remote Sens.* 2019, 11, 957
- Sobrino, J.A.; Jimenez-Munoz, J.C.; Paolini, L. Land surface temperature retrieval from landsat tm 5. *Remote Sens. Environ.* 2004, 90, 434–440.
- Jimenez-Munoz, J.C.; Sobrino, J.A. A generalized single-channel method for retrieving land surface temperature from remote sensing data. *JGR Atmos.* 2003, 108
- Hochreiter, S.; Schmidhuber, J. LSTM can Solve Hard Long Time Lag Problems. In *Proceedings of the NIPS, Denver, CO, USA, 2–5 December 1996*; pp. 473–479
- Foley, Jonathan A., DeFries, Ruth, Asner, Gregory P., Barford, Carol, Bonan, Gordon, & Carpenter, Stephen R. (2005). Global consequences of land use. *Science*, 309(5734).

Meyer, William B., & Turner, II B. (1994). *Turner changes in land use and land cover: A global perspective* (Vol. 4). Cambridge University Press.

Kavzoglu, T., & Mather, P. M. (2003). The use of backpropagating artificial neural networks in land cover classification. *International Journal of Remote Sensing*, 24(23).

Mas, J. F., & Flores, J. J. (2008). The application of artificial neural networks to the analysis of remotely sensed data. *International Journal of Remote Sensing*, 29(3)